Discrete Green's Functions for Harmonic and Biharmonic Inpainting with Sparse Atoms

Sebastian Hoffmann[1], Gerlind Plonka[2], and Joachim Weickert[1]

[1] Mathematical Image Analysis Group
Faculty of Mathematics and Computer Science, Campus E1.7
Saarland University, 66041 Saarbrücken, Germany
{hoffmann,weickert}@mia.uni-saarland.de

[2] Institute for Numerical and Applied Mathematics
University of Göttingen
Lotzestr. 16–18, 37083 Göttingen, Germany
plonka@math.uni-goettingen.de

Abstract. Recent research has shown that inpainting with the Laplace or biharmonic operator has a high potential for image compression, if the stored data is optimised and sufficiently sparse. The goal of our paper is to connect these linear inpainting methods to sparsity concepts. To understand these relations, we explore the theory of Green's functions. In contrast to most work in the mathematical literature, we derive our Green's functions in a discrete setting and on a rectangular image domain with homogeneous Neumann boundary conditions. These discrete Green's functions can be interpreted as columns of the Moore–Penrose inverse of the discretised differential operator. More importantly, they serve as atoms in a dictionary that allows a sparse representation of the inpainting solution. Apart from offering novel theoretical insights, this representation is also simple to implement and computationally efficient if the inpainting data is sparse.

Keywords: inpainting, sparsity, discrete Green's functions, Laplace operator, biharmonic operator.

1 Introduction

Image inpainting with partial differential equations (PDEs) is becoming increasingly important for image compression. For this problem, nonlinear anisotropic diffusion processes have been introduced by Galić et al. in 2005 [7] and have been improved later in [8]. In the meantime, a more sophisticated variant is able to outperform JPEG2000 [19]. Even with a conceptually simpler linear process based e.g. on the Laplace equation, one can achieve remarkable results [15, 12, 17] and beat the quality of state-of-the-art methods for specific types of images [14,

9, 13]. Also the biharmonic equation has been reported to yield very good results [8, 3].

In the present paper, we want to gain theoretical insights on inpainting methods with linear selfadjoint differential operators such as the Laplacian or the biharmonic operator. In particular, we analyse their relation to a very popular idea in modern signal and image analysis, namely sparsity. To this end, we make use of the concept of discrete Green's functions [1, 4]. Green's functions are mainly known from the continuous theory of partial differential equations (PDEs) as a tool to describe the solution of boundary value problems [16]. Most publications on Green's functions focus on continuous differential operators. Digital images, however, reveal a natural discretisation on a regular grid. Moreover, they are given on a rectangular image domain, and it is fairly common to extend image processing operators at the boundaries by mirroring. This motivates us to investigate discrete Green's functions for linear differential operators on a rectangular image domain with homogeneous Neumann boundary conditions. Moreover, we will give an interpretation of the obtained discrete Green's functions in terms of linear algebra. More precisely, we will elaborate the connection to the Moore–Penrose inverse of the discretised differential operator.

The discrete Green's functions that we derive will serve as atoms in a dictionary for inpainting. There is a one-to-one correspondence between each pixel and its corresponding Green's function. Hence, if only a sparse set of pixels is kept, the solution of the discrete inpainting problem can be expressed in a compact way in terms of their Green's functions. We will show that this representation does not only offer novel theoretical insights into the connections between inpainting and sparsity, but also has algorithmic benefits. The main focus of the present paper, however, will be on the theoretical aspect.

The outline of our paper is as follows. First we sketch the continuous and discrete formulations of inpainting with the Laplace and biharmonic equation in Section 2. In the subsequent section we explain the concept of discrete Green's functions and their use for a sparse representation of the solution of the inpainting problems. Numerical advantages of our Green's function framework are discussed in Section 4. Our paper is concluded with a summary in Section 5.

2   Laplace and Biharmonic Inpainting

2.1   Continuous Inpainting Models

Let $\Omega \subset \mathbb{R}^2$ denote a rectangular image domain and $f : \Omega \to \mathbb{R}$ a greyscale image. If this image is only known at some subset $\Omega_K \subset \Omega$, one can try to fill in the missing information by solving the Laplace equation

$$-\boldsymbol{\Delta} u = 0 \qquad \text{on } \Omega \setminus \Omega_K \tag{1}$$

with homogeneous Neumann boundary conditions:

$$\partial_n u = 0 \qquad \text{on } \partial\Omega, \tag{2}$$

where ∂_n denotes the derivative normal to the boundaries. Moreover, the known data set provides Dirichlet boundary conditions:

$$u = f \qquad \text{on } \Omega_K. \tag{3}$$

As an alternative to the Laplace equation, one can also consider higher-order differential operators leading e.g. to the biharmonic equation:

$$\boldsymbol{\Delta}^2 u = 0 \qquad \text{on } \Omega \setminus \Omega_K. \tag{4}$$

Both models have in common that they use linear selfadjoint differential operators. These properties will be useful for our later analysis. From a practical viewpoint they are attractive, since they are parameter-free and give rise to relatively easy implementations.

2.2 Discrete Inpainting Models

Digital images reveal a discretisation on an equispaced rectangular grid. Thus, it is natural to use finite difference discretisations of the beforementioned continuous inpainting processes. We consider a regular two-dimensional grid $\Gamma = \{0, \ldots, M-1\} \times \{0, \ldots, N-1\}$ with grid size h. The value of a discrete image $\boldsymbol{f}$ at a grid point $(i, j) \in \Gamma$ is denoted by $f_{i,j}$. The subset $K \subset \Gamma$ denotes the grid points where the discrete inpainting data is known. We call them mask points. At the locations $\Gamma \backslash K$ where the data is unknown, we seek the inpainting solution $\boldsymbol{u}$ by solving a discrete problem of type

$$(\boldsymbol{Du})_{i,j} = 0 \qquad\qquad \text{for } (i, j) \in \Gamma \backslash K, \tag{5}$$

$$u_{i,j} = f_{i,j} \qquad\qquad \text{for } (i, j) \in K. \tag{6}$$

Here, $\boldsymbol{D}$ can be seen as an inpainting operator. We mainly focus on the following two choices. On the one hand, we consider $\boldsymbol{D} = -\boldsymbol{L}$, where $\boldsymbol{L}$ is the discrete Laplace operator (harmonic operator) on Γ fulfilling homogeneous Neumann boundary conditions at the image boundaries. For the inner grid points its stencil notation is given by

$$\frac{1}{h^2} \begin{array}{|c|c|c|} \hline 0 & 1 & 0 \\ \hline 1 & \text{-4} & 1 \\ \hline 0 & 1 & 0 \\ \hline \end{array} \ .$$

The homogeneous Neumann boundary conditions are incorporated by mirroring the image at the boundaries and by using the above stencil also for the boundary grid points. The resulting inpainting process is also known as homogeneous diffusion inpainting. In [14], the existence and uniqueness of the discrete inpainting solution for the Laplace operator has been shown. On the other hand, we will also consider the biharmonic operator, i.e. $\boldsymbol{D} = \boldsymbol{B} := \boldsymbol{L}^2$.

Typically, the inpainting solution is found by solving the discrete problem directly. This can be done with iterative methods such as a fast explicit diffusion (FED) scheme [11] or bidirectional multigrid approaches [14]. In the present paper we want to study how the solution can be obtained in a noniterative way by means of discrete Green's functions.

2.3   Eigenvalues and Eigenvectors of the Discrete Operators

For our later analysis it is useful to represent the discrete differential operators $-\boldsymbol{L}$ and $\boldsymbol{B}$ in terms of their eigenvalues and eigenvectors. The following theorem provides the required information. It extends 1D results that can be found for example in [20] to the two-dimensional setting.

Theorem 1 (Eigenvalues and Eigenvectors of the Discrete Operators).
The orthonormal set of eigenvectors of $-\boldsymbol{L}$ *as well as of* $\boldsymbol{B}$ *is given by*

$$(\boldsymbol{v}_{m,n})_{i,j} = \begin{cases} \sqrt{\frac{1}{MN}} & \text{if } m = n = 0, \\ \sqrt{\frac{2}{MN}} \cdot \cos\left(\mu\tilde{i}\right) \cdot \cos\left(\nu\tilde{j}\right) & \text{if either } m = 0 \text{ or } n = 0, \\ \sqrt{\frac{4}{MN}} \cdot \cos\left(\mu\tilde{i}\right) \cdot \cos\left(\nu\tilde{j}\right) & \text{if } m > 0 \text{ and } n > 0, \end{cases} \quad (7)$$

with $(m, n) \in \Gamma$, $\mu := \frac{m\pi}{M}$, $\nu := \frac{n\pi}{N}$, $\tilde{i} := (i + \frac{1}{2})$, *and* $\tilde{j} := (j + \frac{1}{2})$.
The corresponding eigenvalues for $-\boldsymbol{L}$ *are*

$$\lambda_{m,n}^{-L} = \frac{4}{h^2}\left(\sin^2\left(\frac{\mu}{2}\right) + \sin^2\left(\frac{\nu}{2}\right)\right). \quad (8)$$

The eigenalues of the discrete biharmonic operator $\boldsymbol{B}$ *read as*

$$\lambda_{m,n}^{B} = \left(\lambda_{m,n}^{-L}\right)^2 \quad (9)$$

Proof. While this eigenstructure may not appear obvious, proving its correctness is fairly straightforward: One has to check that $-\boldsymbol{L}\boldsymbol{v}_{m,n} = \lambda_{m,n}^{-L}\boldsymbol{v}_{m,n}$ and $\boldsymbol{B}\boldsymbol{v}_{m,n} = \lambda_{m,n}^{B}\boldsymbol{v}_{m,n}$ hold true for all $(m, n) \in \Gamma$ and that the homogeneous Neumann boundary conditions are fulfilled. Additionally, one has to show the orthonormality of the set of eigenvectors. $\square$

We observe that both operators are singular, since the eigenvalues $\lambda_{0,0}^{-L}$ and $\lambda_{0,0}^{B}$ vanish. This will complicate some of our discussions on discrete Green's functions in the next section.

3   Discrete Green's Functions

After the preceding discussions we are in a position to introduce the concept of discrete Green's functions. First, we discuss the basic structure before we sketch relations to linear algebra and specific applications to our inpainting problem.

3.1   Basic Structure

Let us study a general discrete problem of the following type:

$$\boldsymbol{D}\boldsymbol{u} = \boldsymbol{a}. \quad (10)$$

Thereby $\boldsymbol{u} \in \mathbb{R}^{M \times N}$ is the unknown image, $\boldsymbol{a} \in \mathbb{R}^{M \times N}$ is a prescribed right hand side, and $\boldsymbol{D} \in \mathbb{R}^{(M \times N) \times (M \times N)}$ a given symmetric discrete linear differential operator incorporating homogeneous Neumann boundary conditions.

The solvability of this problem can be investigated with the so called Fredholm alternative, which is known from the theory of differential equations; see e.g. [5]:

Theorem 2 (Fredholm Alternative). *If $\boldsymbol{D}$ is invertible, then the solution $\boldsymbol{u}$ of the discrete problem (10) exists and is unique. Otherwise, assuming that $\boldsymbol{D}^{\top}$ possesses the single eigenvalue 0 with the corresponding eigenvector $\boldsymbol{v} \in \mathbb{R}^{M \times N}$, there exist infinitely many solutions if*

$$\langle \boldsymbol{v}, \boldsymbol{a} \rangle = 0, \tag{11}$$

and there exists no solution at all if

$$\langle \boldsymbol{v}, \boldsymbol{a} \rangle \neq 0. \tag{12}$$

Here, the Euclidean inner product is defined as $\langle \boldsymbol{a}, \boldsymbol{b} \rangle = \sum_{(i,j) \in \Gamma} a_{i,j} b_{i,j}$. Let us assume that $\boldsymbol{a}$ in (10) is chosen such that there exists a solution $\boldsymbol{u}$. A standard approach to find this solution is to solve the linear system of equations directly. Instead, another promising approach is to express the solution by means of Green's functions. The Green's function can be considered as the influence of an impulse at a point (k, ℓ) on the complete image. Assuming that $\boldsymbol{D}$ is invertible, the discrete Green's function $\boldsymbol{g}_{k,\ell}$ corresponding to a point $(k, \ell) \in \Gamma$ for a given discrete problem is defined as the solution of

$$(\boldsymbol{D}\boldsymbol{g}_{k,\ell})_{i,j} = \delta_{(k,\ell),(i,j)} \qquad \text{for } (i,j) \in \Gamma, \tag{13}$$

where the Kronecker delta function is defined as

$$\delta_{(k,\ell),(i,j)} = \begin{cases} 1 & \text{if } (i,j) = (k,\ell), \\ 0 & \text{if } (i,j) \neq (k,\ell). \end{cases} \tag{14}$$

Otherwise, if $\boldsymbol{D}$ possesses the single eigenvalue 0 and if $\boldsymbol{v}$ is the corresponding eigenvector of $\boldsymbol{D}^{\top}$, we can still obtain Green's functions by the following modification. The infinitely many discrete Green's functions for a point $(k, \ell) \in \Gamma$ are now defined as solutions of

$$(\boldsymbol{D}\boldsymbol{g}_{k,\ell})_{i,j} = \delta_{(k,\ell),(i,j)} - \frac{v_{i,j} \cdot v_{k,\ell}}{\langle \boldsymbol{v}, \boldsymbol{v} \rangle} \qquad \text{for } (i,j) \in \Gamma. \tag{15}$$

Indeed, the right hand side of (15) (in vector notation) now satisfies the solvability condition (11):

$$\left\langle \boldsymbol{v},\ \boldsymbol{\delta}_{k,\ell} - \frac{v_{k,\ell}}{\langle \boldsymbol{v}, \boldsymbol{v} \rangle} \boldsymbol{v} \right\rangle = v_{k,\ell} - v_{k,\ell} = 0. \tag{16}$$

3.2   Interpretation as Moore–Penrose Inverse

The Fredholm alternative can also be expressed in terms of linear algebra. To this end, we reshape the image matrices $\boldsymbol{u}$, $\boldsymbol{a}$ to vectors of length MN using the operation $\text{col} : \mathbb{R}^{M \times N} \to \mathbb{R}^{MN}$, and $\boldsymbol{D}$ to a symmetric $(MN \times MN)$-matrix $\boldsymbol{D}_{MN}$. Then, (10) transfers to a linear system $\boldsymbol{D}_{MN} \, \text{col}\,(\boldsymbol{u}) = \text{col}\,(\boldsymbol{a})$ of size MN. This system is uniquely solvable, if and only if $\boldsymbol{D}_{MN}$ is invertible. If $\text{rank}(\boldsymbol{D}_{MN}) = MN - 1$, then (10) possesses either infinitely many solutions if $\text{rank}(\boldsymbol{D}_{MN}) = \text{rank}(\boldsymbol{D}_{MN}, \text{col}\,(\boldsymbol{a}))$, or no solution if $\text{rank}(\boldsymbol{D}_{MN}) < \text{rank}(\boldsymbol{D}_{MN}, \text{col}\,(\boldsymbol{a}))$.

Assuming that $\boldsymbol{D}_{MN}$ is invertible, the discrete Green's function defined in (13) can be expressed as the solution of

$$\boldsymbol{D}_{MN} \, \boldsymbol{G}_{MN} = \boldsymbol{I}_{MN}, \tag{17}$$

where $\boldsymbol{I}_{MN}$ denotes the identity matrix of size $MN \times MN$ and $\boldsymbol{G}_{MN} \in \mathbb{R}^{MN \times MN}$ the matrix that contains the discrete Green's functions $\boldsymbol{g}_{k,\ell}$ as columns.

If $\text{rank}(\boldsymbol{D}_{MN}) = MN - 1$ then there exist infinitely many Green's functions, and (15) leads to:

$$\boldsymbol{D}_{MN} \, \boldsymbol{G}_{MN} = \boldsymbol{I}_{MN} - \frac{1}{\langle \boldsymbol{v}, \boldsymbol{v} \rangle} (\text{col}\,(\boldsymbol{v}))(\text{col}\,(\boldsymbol{v}))^{\top}. \tag{18}$$

In the following theorem, we introduce a useful additional constraint that creates a unique solution and allows to relate discrete Green's functions to the Moore–Penrose inverse of their discrete differential operator. The Moore–Penrose inverse aims at generalising the inverse of a matrix such that it is also applicable to singular matrices [10].

Theorem 3 (Discrete Green's Functions and Moore–Penrose Inverse).
Let $\text{col}\,(\boldsymbol{v})$ denote the eigenvector to the singular eigenvalue of $\boldsymbol{D}_{MN}$. If the discrete Green's functions $\boldsymbol{g}_{k,\ell}$ satisfy the additional constraint

$$\langle \boldsymbol{v}, \boldsymbol{g}_{k,\ell} \rangle = 0 \qquad \text{for all } (k, \ell) \in \Gamma, \tag{19}$$

then they are given by the columns of the Moore–Penrose inverse of $\boldsymbol{D}_{MN}$.

Proof. To verify that $\boldsymbol{G}_{MN}$ is the Moore–Penrose inverse of $\boldsymbol{D}_{MN}$, we have to check the following properties (cf. [10]):

(i) $\boldsymbol{D}_{MN}\boldsymbol{G}_{MN}\boldsymbol{D}_{MN} = \boldsymbol{D}_{MN}$
(ii) $\boldsymbol{G}_{MN}\boldsymbol{D}_{MN}\boldsymbol{G}_{MN} = \boldsymbol{G}_{MN}$
(iii) $\boldsymbol{D}_{MN}\boldsymbol{G}_{MN}$ is symmetric.
(iv) $\boldsymbol{G}_{MN}\boldsymbol{D}_{MN}$ is symmetric.

Since $\text{col}\,(\boldsymbol{v})$ is an eigenvector of $\boldsymbol{D}_{MN}$ to the eigenvalue 0, we have

$$(\text{col}\,(\boldsymbol{v}))^{\top} \boldsymbol{D}_{MN} = \boldsymbol{0}^{\top}. \tag{20}$$

Thus, together with (18), it follows that

$$\boldsymbol{D}_{MN}\boldsymbol{G}_{MN}\boldsymbol{D}_{MN} = \left(\boldsymbol{I}_{MN} - \frac{1}{\langle \boldsymbol{v}, \boldsymbol{v}\rangle}(\text{col}\,(\boldsymbol{v}))(\text{col}\,(\boldsymbol{v}))^{\top}\right)\boldsymbol{D}_{MN} = \boldsymbol{D}_{MN} \quad (21)$$

and

$$\boldsymbol{G}_{MN}\boldsymbol{D}_{MN}\boldsymbol{G}_{MN} = \boldsymbol{G}_{MN} - \frac{1}{\langle \boldsymbol{v}, \boldsymbol{v}\rangle}\boldsymbol{G}_{MN}(\text{col}\,(\boldsymbol{v}))(\text{col}\,(\boldsymbol{v}))^{\top}. \quad (22)$$

The condition $\langle \boldsymbol{v}, \boldsymbol{g}_{k,\ell}\rangle = 0$ implies $\boldsymbol{G}_{MN}(\text{col}\,(\boldsymbol{v})) = \boldsymbol{0}$, and hence

$$\boldsymbol{G}_{MN}\boldsymbol{D}_{MN}\boldsymbol{G}_{MN} = \boldsymbol{G}_{MN}. \quad (23)$$

From (18) it is evident that $\boldsymbol{D}_{MN}\boldsymbol{G}_{MN}$ is symmetric. Let us now show that also $\boldsymbol{G}_{MN}\boldsymbol{D}_{MN}$ is symmetric. Due to the symmetry of $\boldsymbol{D}_{MN}$, we can diagonalise it and write

$$\boldsymbol{D}_{MN} = \boldsymbol{V}\boldsymbol{S}\boldsymbol{V}^{\top} \quad (24)$$

with a diagonal matrix $\boldsymbol{S}$ and an orthogonal matrix $\boldsymbol{V}$. Since $\boldsymbol{D}_{MN}$ contains a singular eigenvalue, we obtain the Moore–Penrose inverse $\boldsymbol{G}_{MN}$ as

$$\boldsymbol{G}_{MN} = \boldsymbol{D}_{MN}^{+} = \boldsymbol{V}\boldsymbol{S}^{+}\boldsymbol{V}^{\top}. \quad (25)$$

The matrix $\boldsymbol{S}^{+}$ contains the reciprocal of the eigenvalues except for the zero eigenvalue that remains 0. Furthermore, as $\boldsymbol{V}$ is orthogonal, we obtain

$$\boldsymbol{G}_{MN}\boldsymbol{D}_{MN} = \left(\boldsymbol{V}\boldsymbol{S}^{+}\boldsymbol{V}^{\top}\right)\left(\boldsymbol{V}\boldsymbol{S}\boldsymbol{V}^{\top}\right) = \boldsymbol{V}\boldsymbol{S}^{+}\boldsymbol{S}\boldsymbol{V}^{\top} \quad (26)$$

as well as

$$\left(\boldsymbol{G}_{MN}\boldsymbol{D}_{MN}\right)^{\top} = \left(\boldsymbol{V}\boldsymbol{S}\boldsymbol{V}^{\top}\right)^{\top}\left(\boldsymbol{V}\boldsymbol{S}^{+}\boldsymbol{V}^{\top}\right)^{\top} \quad (27)$$

$$= \boldsymbol{V}\boldsymbol{S}^{\top}\left(\boldsymbol{S}^{+}\right)^{\top}\boldsymbol{V}^{\top} = \boldsymbol{V}\boldsymbol{S}^{+}\boldsymbol{S}\boldsymbol{V}^{\top} \quad (28)$$

$$= \boldsymbol{G}_{MN}\boldsymbol{D}_{MN}. \quad (29)$$

Thus, $\boldsymbol{G}_{MN}\boldsymbol{D}_{MN}$ is symmetric, too. □

3.3   Representing Solutions with Green's Functions

Knowing the Green's functions for all $(k,\ell) \in \Gamma$, the following theorem can be formulated [6]:

Theorem 4 (Analytic Solution). *The solution $\boldsymbol{u}$ of the discrete problem (10) is given by*

$$\boldsymbol{u} = \sum_{(k,\ell)\in\Gamma} a_{k,\ell}\,\boldsymbol{g}_{k,\ell} \quad (30)$$

where in case of a singular operator $\boldsymbol{D}$ the solvability condition (11) is assumed to be satisfied, and the solution based on the Green's functions is no longer unique.

In practice, it is often not straightforward to determine the Green's functions, since they depend on the domain as well as on the boundary conditions. There exist some designated approaches for specific problem settings [16]. The probably most promising technique is the so-called *method of eigenfunction expansion* [16] for the continuous case. In the discrete setting, the discrete Green's functions are expressed in terms of the eigenvectors and corresponding eigenvalues of $\boldsymbol{D}$ (cf. [1]). Let us now study this approach in detail.

3.4   Constructing Discrete Green's Functions for our Operators

Let us now apply our theory on the discrete Laplace or biharmonic operator. To this end, we recall that both operators $-\boldsymbol{L}$ and $\boldsymbol{B}$ have a zero eigenvalue $\lambda_{0,0}$. It belongs to the constant eigenvector $\boldsymbol{v}_{0,0}$ with entries $1/\sqrt{MN}$. Thus, we know from Section 3 that in a point $(k,\ell) \in \Gamma$, the Green's function $\boldsymbol{g}_{k,\ell}$ for both operators is not unique. It satisfies the following system of equations:

$$(\boldsymbol{D}\boldsymbol{g}_{k,\ell})_{i,j} = \delta_{(k,\ell),(i,j)} - \frac{1}{MN} \qquad \text{for } (i,j) \in \Gamma \tag{31}$$

with $\boldsymbol{D} = -\boldsymbol{L}$ or $\boldsymbol{D} = \boldsymbol{B}$, respectively. The theorem below states the solution in a closed form:

Theorem 5 (Discrete Green's Functions). *In a point $(k,\ell) \in \Gamma$ the discrete Green's functions for the matrix $\boldsymbol{D} = -\boldsymbol{L}$ or $\boldsymbol{D} = \boldsymbol{B}$ are given by*

$$(\boldsymbol{g}_{k,\ell}^c)_{i,j} = \sum_{\substack{m=0 \\ (m,n)\neq(0,0)}}^{M-1} \sum_{n=0}^{N-1} \left[\frac{1}{\lambda_{m,n}} \cdot (\boldsymbol{v}_{m,n})_{k,\ell} \cdot (\boldsymbol{v}_{m,n})_{i,j} \right] + c, \tag{32}$$

where $\lambda_{m,n}$ are the eigenvalues corresponding to the eigenvectors $\boldsymbol{v}_{m,n}$ of $\boldsymbol{D}$, and the constant $c \in \mathbb{R}$ can be chosen arbitrarily.

Proof. Following [1], we express the Green's function in terms of the orthonormal eigenvectors:

$$\boldsymbol{g}_{k,\ell} = \sum_{m=0}^{M-1} \sum_{n=0}^{N-1} c_{m,n} \boldsymbol{v}_{m,n} \tag{33}$$

with coefficients $c_{m,n} \in \mathbb{R}$. Plugging this into (31) yields

$$\sum_{m=0}^{M-1} \sum_{n=0}^{N-1} c_{m,n} \lambda_{m,n} (\boldsymbol{v}_{m,n})_{i,j} = \delta_{(k,\ell),(i,j)} - \frac{1}{MN}. \tag{34}$$

After multiplying both sides with $(\boldsymbol{v}_{m',n'})_{i,j}$ for fixed $(m',n') \in \Gamma$, and summing up over all pixels $(i,j) \in \Gamma$, we have

$$c_{m',n'} \lambda_{m',n'} = (\boldsymbol{v}_{m',n'})_{k,\ell} - \frac{1}{MN} \sum_{(i,j)\in\Gamma} (\boldsymbol{v}_{m',n'})_{i,j}. \tag{35}$$
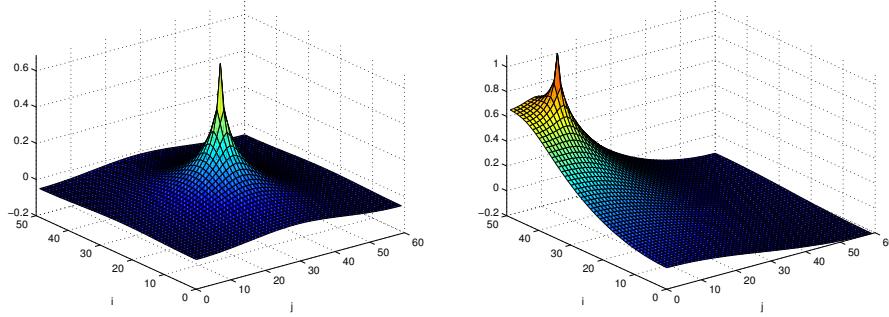
Fig. 1. Example of discrete Green's functions for the negative Laplacian with homogeneous Neumann boundary conditions on an image with 50×60 pixels. **Left: $g^0_{25,30}$. Right: $g^0_{45,10}$**
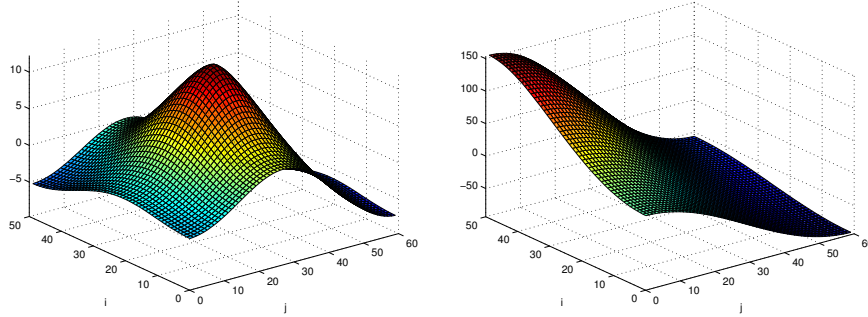

.

Fig. 2. Example of discrete Green's functions for the biharmonic operator with homogeneous Neumann boundary conditions on an image with 50×60 pixels. **Left: $g^0_{25,30}$. Right: $g^0_{45,10}$**

.

For $m' = n' = 0$, the eigenvalue $\lambda_{0,0}$ as well as the right hand side become 0 by (7). Thus, $c_{0,0}$ can be chosen arbitrarily. This means that the Green's function is unique up to a constant c. For $m' > 0$ or $n' > 0$, we obtain

$$c_{m,n} = \frac{1}{\lambda_{m,n}} \left(\boldsymbol{v}_{m,n} \right)_{k,\ell}. \tag{36}$$

This concludes the proof. □

We specify a canonic representative $\boldsymbol{g}^0_{k,\ell}$ by setting the constant $c := 0$. As the eigenvectors $\boldsymbol{v}_{m,n}$ with $(m, n) \neq (0, 0)$ of the discrete operator are orthogonal to $\boldsymbol{v}_{0,0}$, this is equivalent to assuming $\langle \boldsymbol{g}^0_{k,\ell}, \boldsymbol{v}_{0,0} \rangle = 0$. This shows that the obtained Green's functions $\boldsymbol{g}^0_{k,\ell}$ have mean value zero. Moreover, we can apply Theorem 3 and see that they build the Moore–Penrose inverse of $\boldsymbol{D}$. Example plots of Green's functions are depicted in Figure 1 and 2.

In practice, we can exploit the symmetry of the rectangular image domain to reduce the effort for computing all discrete Green's functions by a factor of 4: Once the Green's function is computed for a specific source point $(k, \ell) \in \Gamma$, the Green's functions for the source points $(M - k, \ell)$, $(k, N - \ell)$, and $(M - k, N - \ell)$ can be obtained by mirroring $\boldsymbol{g}_{k,\ell}^0$ along the x axis, the y axis and both axes.

3.5   Inpainting with Green's Functions

We want to use the Green's functions to find an exact solution of the discrete inpainting problem. Therefore, the trick is to rewrite the problem such that it has the form as in (10). We construct a right hand side $\boldsymbol{a}$ such that it is zero at all non-mask points, while its values at all mask points $(i, j) \in K$ must be determined later. As a result, the problem reads as

$$\boldsymbol{D}\boldsymbol{u} = \boldsymbol{a} \tag{37}$$

subject to

$$u_{i,j} = f_{i,j} \qquad \text{if } (i, j) \in K, \tag{38}$$
$$a_{i,j} = 0 \qquad \text{if } (i, j) \in \Gamma \backslash K. \tag{39}$$

Assuming that $\langle \boldsymbol{v}_{0,0}, \boldsymbol{a} \rangle = 0$ we can write the solution $\boldsymbol{u}$ of (37) as

$$u_{i,j} = \sum_{(k,\ell) \in \Gamma} a_{k,\ell} \cdot (\boldsymbol{g}_{k,\ell}^0)_{i,j} + c \tag{40}$$

with the discrete canonic Green's functions $\boldsymbol{g}_{k,\ell}^0$ $((k, \ell) \in \Gamma)$ and an unknown constant c, comprising all constants of the individual Green's functions. As by (39) the entries of $\boldsymbol{a}$ vanish at all non-mask points, (40) can be simplified to

$$u_{i,j} = \sum_{(k,\ell) \in K} a_{k,\ell} \cdot (\boldsymbol{g}_{k,\ell}^0)_{i,j} + c. \tag{41}$$

This representation shows that the inpainting solution can be composed by a small number of atoms, namely the discrete Green's functions corresponding to the mask pixels. Thus, the discrete Green's functions $\boldsymbol{g}_{k,\ell}^0$ corresponding to $(k, \ell) \in K$ can be seen as a generating system for the space of all inpainting solutions on $\Gamma \setminus K$ (with mean value zero on Γ).

It remains to find the unknown coefficients c and $a_{k,\ell}$, $(k, \ell) \in K$. They are determined by (38). Together with the solvability condition (11) within the Fredholm alternative,

$$\langle \boldsymbol{v}_{0,0}, \boldsymbol{a} \rangle = 0 \qquad \Longleftrightarrow \qquad \sum_{(k,\ell) \in K} a_{k,\ell} = 0, \tag{42}$$

we can specify the inpainting result uniquely. Denoting the 2D pixel indices of the mask points by $m_1, \ldots, m_L$, with $L := |K|$, we can formulate the linear

---

Algorithm 1. Inpainting with Green's functions.

Input: Image $\boldsymbol{f}$ at specified mask K.

1. For all $(k, \ell) \in K$, compute the corresponding canonic Green's function $\boldsymbol{g}^0_{k,\ell}$ using Theorem 5.
2. Compute the unknown coefficients of $\boldsymbol{a}$ and c by solving (43).
3. Obtain the solution $\boldsymbol{u}$ as the superposition given in (41).

Output: Inpainting solution $\boldsymbol{u}$.

---

system of equations for finding the unknown values of $\boldsymbol{a}$ and c:

$$\begin{pmatrix} (\boldsymbol{g}^0_{m_1})_{m_1} & (\boldsymbol{g}^0_{m_2})_{m_1} & \cdots & (\boldsymbol{g}^0_{m_L})_{m_1} & 1 \\ (\boldsymbol{g}^0_{m_1})_{m_2} & (\boldsymbol{g}^0_{m_2})_{m_2} & \cdots & (\boldsymbol{g}^0_{m_L})_{m_2} & 1 \\ \vdots & \vdots & \ddots & \vdots & \vdots \\ (\boldsymbol{g}^0_{m_1})_{m_L} & (\boldsymbol{g}^0_{m_2})_{m_L} & \cdots & (\boldsymbol{g}^0_{m_L})_{m_L} & 1 \\ 1 & 1 & \cdots & 1 & 0 \end{pmatrix} \begin{pmatrix} a_{m_1} \\ a_{m_2} \\ \vdots \\ a_{m_L} \\ c \end{pmatrix} = \begin{pmatrix} f_{m_1} \\ f_{m_2} \\ \vdots \\ f_{m_L} \\ 0 \end{pmatrix}. \tag{43}$$

For solving this system of equations, we recommend the QR algorithm since it does not create error accumulations [18]. Once the values for c and $a_{m_1},...,a_{m_L}$ are computed, the inpainting solution $\boldsymbol{u}$ is represented exactly with (41). For the reader's convenience, Algorithm 1. summarises the full workflow.

A decisive advantage of our inpainting algorithm with Green's functions is that it reveals the influence of each mask point on the overall inpainting result: This influence is described by the respective Green's function. It is clear that the complexity for finding a solution increases with the number of mask points. Interestingly, this is different to the standard approach of solving the discrete inpainting problem iteratively, where it is computationally more expensive to find a solution for a sparse mask: In the latter case, it typically takes more time to diffuse the information at the mask points over the complete image. In contrast, our new approach can compute the solution much faster if the specified data is sparse. For image compression applications this can be a relevant scenario.

4   Experiments

Although the main goal of our paper is to emphasise the theoretical advantages of Green's functions as a tool to understand the connections between PDE-based inpainting and sparsity, our framework can also offer practical advantages. This shall be illustrated by an application in the context of image compression with PDEs. In order to reconstruct an image in the decoding step, we have to solve inpainting problems. If they use the Laplacian or biharmonic operator, we propose to refrain from storing the greyvalues at all mask pixels and rather store the coefficients c and $a_{m_1},...,a_{m_{L-1}}$ instead. Note that the missing coefficient a_{m_L} can be recovered from these coefficients with the help of the solvability condition (42). The computation of the Green's functions can be performed

Table 1. Runtime comparison for inpainting with the Laplace operator. The CPU time is given in seconds.

mask density	0.01%	0.5%	1%	2%	4%	8%	16%
multigrid (max. error 0.5)	0.425	0.306	0.305	0.305	0.264	0.263	0.216
multigrid (max. error 0.05)	0.777	0.855	0.581	0.579	0.263	0.263	0.216
multigrid (max. error 0.005)	11.331	2.238	1.685	0.857	0.742	0.502	0.216
our approach	0.001	0.037	0.073	0.143	0.293	0.585	1.179

Table 2. Runtime comparison for inpainting with the biharmonic operator. The CPU time is given in seconds.

mask density	0.01%	0.5%	1%	2%	4%	8%	16%
multigrid (max. error 0.5)	0.691	0.463	0.464	0.462	0.382	0.382	0.305
multigrid (max. error 0.05)	0.688	0.876	0.875	0.874	0.382	0.383	0.305
multigrid (max. error 0.005)	5.312	2.114	1.287	1.306	0.725	0.382	0.305
our approach	0.001	0.037	0.074	0.148	0.298	0.597	1.181

offline before storing them on the hard disk. This has the advantage that they do not have to be recomputed every time they are needed. As a result, we obtain a very efficient decoding for sparse masks where the inpainting result is computed by a simple superposition of Green's functions.

To evaluate this algorithm for inpainting with the Laplace or biharmonic operator, we compare it with bidirectional multigrid methods. These sophisticated numerical algorithms belong to the most efficient techniques that are used for this purpose; see e.g. [14]. As a model problem, we consider an image of size 256×256 pixels with greyvalues in the range between 0 and 255. Moreover, we use randomly sampled mask points with varying density. Table 1 juxtaposes the runtimes of our Green's function algorithm and bidirectional multigrid methods with two different accuracy levels for the Laplace operator. Corresponding comparisons for the biharmonic operator are presented in Table 2. We use C implementations on an Intel Xeon quadcore architecture with 3.2 GHz and 24 GB memory. For more details on the multigrid implementation, we refer to [14].

We observe that our Green's function approach gives favourable results if the mask density is low and high accuracy is needed. In the context of depth map compression for example, one usually deals with very sparse masks as only few data points suffice to represent smooth transitions [13]. This shows the practical relevance of the presented algorithm. Note that in contrast to the bidirectional multigrid approach, the Green's function algorithm solves the discrete inpainting problem exactly (up to machine precision). Thus, there is no need for devising appropriate stopping criteria and making decisions on the numerous parameters that are characteristic for multigrid methods. Last but not least, it should be emphasised that the runtime of the Green's function method does not deteriorate when one replaces the Laplace operator by the biharmonic operator (or even higher order linear differential operators). It remains a simple superposition of Green's functions.

5   Conclusion

Since one decade, the paradigms of sparse signal processing and inpainting methods for compact image representations have been enjoying a successful development. Although they often pursue similar goals, it is surprising that this has happened without any interaction. With our paper, we have paved the way for a mutual exchange of ideas.

The key concept for understanding this relation was the notion of discrete Green's functions. They serve as atoms in a dictionary. Only a single atom is needed to describe the global influence of one mask pixel. This allows to reinterpret successful inpainting methods with linear differential operators in terms of sparsity. Moreover, discrete Green's functions also offer an interesting interpretation as columns of the Moore–Penrose pseudoinverse of the discretised (singular) differential operator.

Our framework is fairly general: It is directly applicable to any linear selfadjoint differential operator with a known eigendecomposition. We have illustrated this by means of the Laplace operator with homogeneous Neumann boundary conditions and its biharmonic counterpart.

One important result of our Green's function research is the fact that it allows us to have direct access to the exact solution of the discrete inpainting problem. This may also have practical advantages for PDE-based decoding with sparse inpainting masks. In our ongoing research, we are also exploring applications of Green's functions within the encoding step.

It is worth mentioning that our representation of PDE-based inpainting in terms of Green's functions also connects PDE-based image compression to scattered data interpolation with radial basis functions [2]. Many of these basis functions are given as continuous Green's functions on an unbounded domain. With our research we have taken into account the discreteness of digital images and have incorporated image boundaries in a natural way.

References

1. Berger, J.M., Lasher, G.J.: The use of discrete Green's functions in the numerical solution of Poisson's equation. Illinois Journal of Mathematics 2(4A), 593–607 (Nov 1958)
2. Buhmann, M.D.: Radial Basis Functions. Cambridge University Press, Cambridge, UK (2003)
3. Chen, Y., Ranftl, R., Pock, T.: A bi-level view of inpainting-based image compression. In: Kúkelová, Z., Heller, J. (eds.) Proc. 19th Computer Vision Winter Workshop. Křtiny, Czech Republic (Feb 2014)
4. Chung, F., Yau, S.T.: Discrete Green's functions. Journal of Combinatorial Theory, Series A 91(12), 191–214 (2000)

5. Colton, D.: Partial Differential Equations: An Introduction. Dover, New York (2004)
6. Evans, G., Blackledge, J., Yardley, P.: Analytic Methods for Partial Differential Equations. Springer, London (2000)
7. Galić, I., Weickert, J., Welk, M., Bruhn, A., Belyaev, A., Seidel, H.P.: Towards PDE-based image compression. In: Paragios, N., Faugeras, O., Chan, T., Schnörr, C. (eds.) Variational, Geometric and Level-Set Methods in Computer Vision, Lecture Notes in Computer Science, vol. 3752, pp. 37–48. Springer, Berlin (2005)
8. Galić, I., Weickert, J., Welk, M., Bruhn, A., Belyaev, A., Seidel, H.P.: Image compression with anisotropic diffusion. Journal of Mathematical Imaging and Vision 31(2–3), 255–269 (Jul 2008)
9. Gautier, J., Meur, O.L., Guillemot, C.: Efficient depth map compression based on lossless edge coding and diffusion. In: Picture Coding Symposium. pp. 81–84. Kraków, Poland (May 2012)
10. Golub, G.H., Van Loan, C.F.: Matrix computations. The John Hopkins University Press, New York (1996)
11. Grewenig, S., Weickert, J., Bruhn, A.: From box filtering to fast explicit diffusion. In: Goesele, M., Roth, S., Kuijper, A., Schiele, B., Schindler, K. (eds.) Pattern Recognition, Lecture Notes in Computer Science, vol. 6376, pp. 533–542. Springer, Berlin (2010)
12. Hoeltgen, L., Setzer, S., Weickert, J.: An optimal control approach to find sparse data for Laplace interpolation. In: Heyden, A., Kahl, F., Olsson, C., Oskarsson, M., Tai, X.C. (eds.) Energy Minimization Methods in Computer Vision and Pattern Recognition, Lecture Notes in Computer Science, vol. 8081, pp. 151–164. Springer, Berlin (2013)
13. Hoffmann, S., Mainberger, M., Weickert, J., Puhl, M.: Compression of depth maps with segment-based homogeneous diffusion. In: Kuijper, A., Bredies, K., Pock, T., Bischof, H. (eds.) Scale Space and Variational Methods in Computer Vision, Lecture Notes in Computer Science, vol. 7893, pp. 319–330. Springer, Berlin (2013)
14. Mainberger, M., Bruhn, A., Weickert, J., Forchhammer, S.: Edge-based image compression of cartoon-like images with homogeneous diffusion. Pattern Recognition 44(9), 1859–1873 (Sep 2011)
15. Mainberger, M., Hoffmann, S., Weickert, J., Tang, C.H., Johannsen, D., Neumann, F., Doerr, B.: Optimising spatial and tonal data for homogeneous diffusion inpainting. In: Bruckstein, A.M., ter Haar Romeny, B., Bronstein, A.M., Bronstein, M.M. (eds.) Scale Space and Variational Methods in Computer Vision, Lecture Notes in Computer Science, vol. 6667, pp. 26–37. Springer, Berlin (2012)
16. Melnikov, Y., Melnikov, M.: Green's Functions: Construction and Applications. De Gruyter, Berlin (2012)
17. Ochs, P., Chen, Y., Brox, T., Pock, T.: iPiano: Inertial proximal algorithm for nonconvex optimization. SIAM Journal on Imaging Sciences 7(2), 1388–1419 (2014)
18. Sauer, T.: Numerical Analysis. Pearson Addison Wesley, Boston (2006)
19. Schmaltz, C., Peter, P., Mainberger, M., Ebel, F., Weickert, J., Bruhn, A.: Understanding, optimising, and extending data compression with anisotropic diffusion. International Journal of Computer Vision 108(3), 222–240 (Jul 2014)
20. Strang, G., MacNamara, S.: Functions of difference matrices are Toeplitz plus Hankel. SIAM Review 56(3), 525–546 (2014)